An Overview of Bulk Parametrization and Remote Sensing of Latent Heat Flux in the Tropical Ocean

W. Timothy LIU

M.S. 300-323
Jet Propulsion Laboratory
California Institute of Technology
Pasadena, CA 91109 - U.S.A.

1. INTRODUCTION

The only practical way of determining large-scale air-sea exchanges in momentum, heat and moisture is through the bulk formulae which link the microscale turbulent transfer to macroscale parameters measured routinely. The coefficients used in these formulae were derived and verified with observations taken in moderate wind conditions (4-15 m/s) under near neutral condition. Over large areas in the tropical Pacific, the mean wind is weak (< 3 m/s) and the sea-air humidity difference reaches above 7 g/kg (e.g., Hsiung 1986). The moisture induced buoyancy destabilizes the atmosphere and increases evaporation. The characteristics of the coefficients under these conditions will be discussed

Except near coastal area and in major shipping lanes, meteorological reports are sparse in the tropical ocean. *In situ* measurements are not adequate to delineate the temporal and spatial variabilities of the fluxes. Spaceborne sensors provide repeated and uniform coverage. A method of computing the moisture flux using spaceborne sensors will be described and examples of scientific application will be presented.

2. FORCED CONVECTION

The bulk parameterization formulae are

$$\tau = \rho C_D U^2 \qquad (1a)$$

$$H = \rho c C_H U (T_s - T) \qquad (1b)$$

$$E = \rho C_E U (Q_s - Q) \qquad (1c)$$

where τ is the wind stress, H is the sensible heat flux, E is the moisture flux, ρ is surface air density, c is the isobaric specific heat. The latent heat flux (LE) is the product of E and the latent heat of vaporization. The measurements required are the sea surface temperature (T_s), the wind speed (U), the temperature (T), and the specific humidity (Q) measured on board ships. The specific humidity at the air-sea interface (Q_s) is generally taken to be the saturation value at T_s and Q can be derived from the dew-point temperature measured. The transfer coefficients (C_D, C_H and C_E) used are generally assumed to be constant and determined by regression of spot measurements (10 min to 1 hr time averages at a fixed location). The coefficients, in theory, depends on the reference height, the stability and surface roughness. Liu et al. (1979) developed a model to account for these variabilites.

In the model of Liu et al. (1979), which is a physical approach to bulk parameterization, the three non-dimensional profiles based on similarity theory are solved simultaneously. The similarity relations are,

$$U/U_* = 2.5(z/z_o - \psi_U) = C_D^{-1/2}, \tag{2a}$$

$$(T - T_s)/T_* = 2.2(z/z_T - \psi_T) = C_D^{1/2}C_H^{-1}, \tag{2b}$$

$$(Q - Q_s)/Q_* = 2.2(z/z_Q - \psi_Q) = C_D^{1/2}C_E^{-1}. \tag{2c}$$

By definition, $U*$, $T*$, $Q*$ are function of τ, H, and E. The ψ_U, ψ_T, and ψ_Q are function of the stability parameter (ζ) and can be expressed in terms of the three fluxes. The lower boundary parameters z_o, z_T, and z_Q are functions of τ and fluid properties. The three unknowns τ, H, and E can be determined by solving the three implicit equations. This method is similar to that used by Deardorff (1968) to account for the effects of stability on the values of the transfer coefficients and is equivalent to using (1) with variable coefficients.

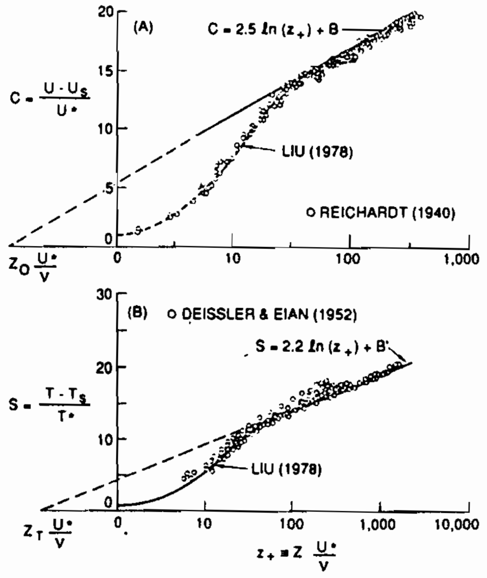

Fig.1 Laboratory measurements of the vertical profiles of (A) velocity and (B) temperature, (from Liu, 1978).

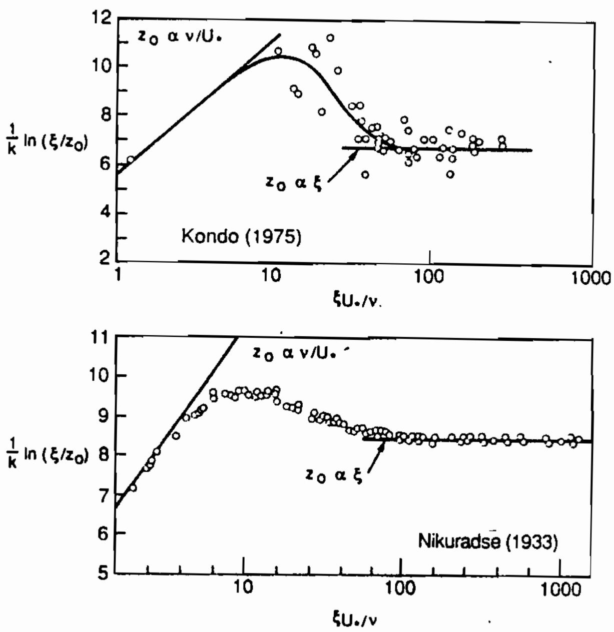

Fig.2 Variation of the roughness parameter in pipe flow (A) and at the sea-air interface (B), (from Liu, 1978).

Under neutral stability ($\psi_U=\psi_T=\psi_Q=0$), the variabilities of the coefficients are governed by the variabilities of z_o, z_T, and z_Q. The three parameters reflect the transport processes near the surface. The velocity and and temperature distributions measured in smooth channels by Reichardt (1940) and Deissler & Eian (1952) are shown in Fig. 1. Away from the surface, the flow is turbulent and the measurements follow a logarithmic law. Near the surface, viscosity and conductivity become important and the profiles agree with the postulation based on a surface renewal model by Liu et al.(1979). The imagery height at which the $U-U_s=0$ along the extrapolaiton of the logarithmic profile is z_o. The interpretation of z_T and z_Q are the same except for temperature and specific humidity. Schlichting (1968) suggested that a surface is aerodynamically rough when the roughness elements penetrate the viscous sublayer and it is smooth if the sublayer covers the roughness elements. The scaling depth of the sublayer is ν/U_*, where ν is the kinematic viscosity. Alternatively, rough flow can be viewed as the state when the local velocity scale and the characteristic scale of the roughness elements, ξ, combined to form a roughness Reynolds Number ($\xi U_*/\nu$) that exceed a critical value. The velocity measurements in pipe flow by Nikuradse (1933) are shown in Fig. 2A. ξ is the actual mean diameter of the the sand-grains used as roughness elements. The measurements of Kondo (1975) at an air-sea interface are shown in Fig. 2B and ξ is the square root of the integral of the one dimensional wave spectrum between two selected frequencies. In smooth flow, $\xi << \nu/U_*$, momentum is mainly transported by viscosity, z_o is proportional to ν/U_*, and, therefore, C_D increases with decreasing U_*. In rough flow, $\xi >> \nu/U_*$, momentum is mainly transported by pressure force on the roughness element and the flow is independent of ν, and z_o is proportional to ξ. In the case of a rough sea surface, ξ increases with wind and, therefore, C_D increases with wind. Charnock (1955) postulated that z_o is proportional to U_*^2/g where g is the acceleration due to gravity.

When the interface is smooth, momentum, heat and water vapor are all transported by molecular processes near the interface and the variations of C_D, C_H, and C_E should share the same characteristics, i.e., increases with decreasing winds. When the roughness of the surface increases, turbulent transport is facilitated and the transfer coefficients increase with wind speed. While momentum can be transported by pressure forces on the roughness elements independent of viscosity, the slow molecular diffusion is the only process which transport heat and mass at the interface. Increase in roughness increases the sheltering effect and the fluid stays longer in contact with the surface before turbulence carries it away. The opposing effects on the C_E is shown in Fig. 3. The thick curve represents C_E at neutral stability from the model of Liu et al. (1979). At low wind speed, it decreases with increasing wind speed, having the characteristics of smooth flow described above. The behavior of C_E at low winds was recently supported by the measurements of Bradley et al. (1989) in the Brismack Sea. As the wind speed increases and the surface becomes rough, the opposing effects of increase stirring and sheltering balance out and the C_E remains rather constant at 1.3×10^{-3} in good agreement the empirical values (shown as dashed lines) by Anderson and Smith (1981) (A&S) and Large and Pond (L&P). The value given by Bunker (1976) (B), however, increases with wind speed, following the characteristics of C_D.

In (2), ψ_U, ψ_T, and ψ_Q are functions of the stability parameter ($\zeta \equiv z/L$), where z is the height and L is the Monin-Obukhov length. The parameter is the ratio of turbulence production by buoyancy to those by shear. Assuming $C_D=C_H=C_Q=C$, it can be approximated (Deardorff, 1968) by

$$\zeta \cong \frac{kgz\,(\Delta T + 0.619\Delta Q)}{\sqrt{C}\;\theta\;U^2} \tag{3a}$$

where k is the von Karman's constant, $\Delta T \equiv T_s - T$, $\Delta Q \equiv Q_s - Q$, and θ is the average absolute temperature. As the flux-profile relations, initially developed over land, are extended over water, the effects of humidity fluctuation on buoyancy is often overlooked. Bunker (1976), for example, tabulated the values of the transfer coefficients according to classes of U and ΔT but not ΔQ. In the extratropical oceans, the effects of humidity fluctuations may be small compared with the effects of temperature fluctuations. But in the tropical oceans, due to the rapid increase of saturation humidity at high temperature (Clausius-Clapeyron Equation), humidity fluctuations can have significant effects on atmospheric stability and the variability of the transfer coefficient. Fig 4 shows the ratio of ζ / ζ_*, where

$$\zeta_* \cong \frac{kgz\,\Delta T}{\sqrt{C}\;\theta\;U^2} \tag{3b}$$

at various T_s and two values of ΔT, assuming $C=1.3 \times 10^{-3}$, U=7 m/s and a relative humidity of 80%. It is obvious that the error for omitting ΔQ can be larger than 50% over warm water (>25°C). In the western tropical Pacific and eastern Indian Ocean, with a typical wind speed of 4 m/s, and a typical sea-air humidity difference of 6 g/kg (Hsiung, 1986), the coefficient is approximately 1.8×10^{-3} as shown in Fig. 3. This will give a latent heat flux approximately 40% higher than the value given by a neutral coefficient of 1.3×10^{-3}. The typical ΔT may be small and the temperature induced buoyancy alone cannot adequately account for the stability effect on C_E.

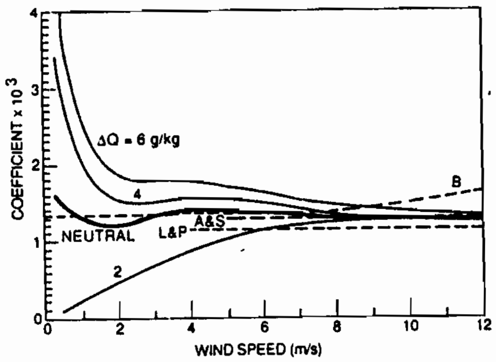

Fig.3 Variation of the moisture transfer coefficient with wind and sea-air humidity difference computed with model of Liu et al. (1989), with the thick line representing values at neutral stability.

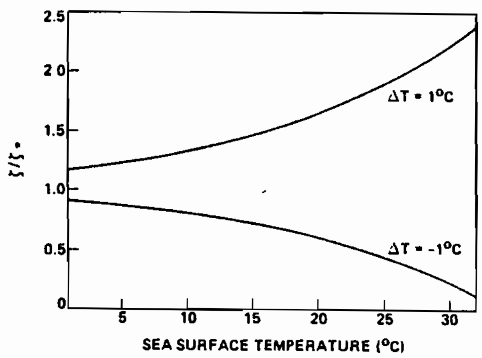

Fig 4. The ratio of the stability parameter including humidity effects to the stability parameter excluding humidity effects as a function of temperature for two cases of sea-air temperature differences (ΔT).

3. FREE CONVECTION

The bulk formula (1) imply that there is no heat and moisture transfer at zero wind speed which, of course, is not true. Convection caused by buoyancy force as a result of heating or concentration gradient will transport heat and moisture. The similarity profiles (2) are not valid under free convection when buoyancy dominates over shear in turbulence production. In open oceans, free convection is rare and is not well studied. However, there are many studies of free convection of homogeneous fluids, particularly in laboratory Liu (1984) gave a detailed review. Krishnamurti (1973) showed that the circulation in a fluid goes from laminar to fully turbulent as the Raleigh number for temperature ($Ra_T \equiv \alpha g \Delta T d^3/(\kappa_T \nu)$) increases. In the definition of Ra_T, α is the coefficient of thermal expansion and κ_T is the thermal conductivity. When the flow is fully turbulent, theoretical and empirical studies suggest that the heat transport is governed by

$$Nu = A\ Ra_T^{1/3} \tag{4}$$

where $Nu \equiv Hd/(\rho c \kappa_T \Delta T)$ is the Nusselt number, and A depends on the Prandtl Number $Pr = \nu/\kappa_T$. Fig. 5, from Liu (1974), shows the results of an experiment with a deep well-insulated tank of water under an evaporating free surface Surface heat flux is equated to water heat loss derived from calorimetry. Water surface temperature was measured both by an Barnes PRT-5 radiometer mounted above the tank and by moving a 25 micron diameter resistant film probe across the surface. The bulk temperature was measured by a thermometer. The 110 pairs of data have a correlation coefficients of 0.997 and the linear fit corresponds to a relation $Nu = 0.156 Ra_T$. Eqn (4) can be reduced to

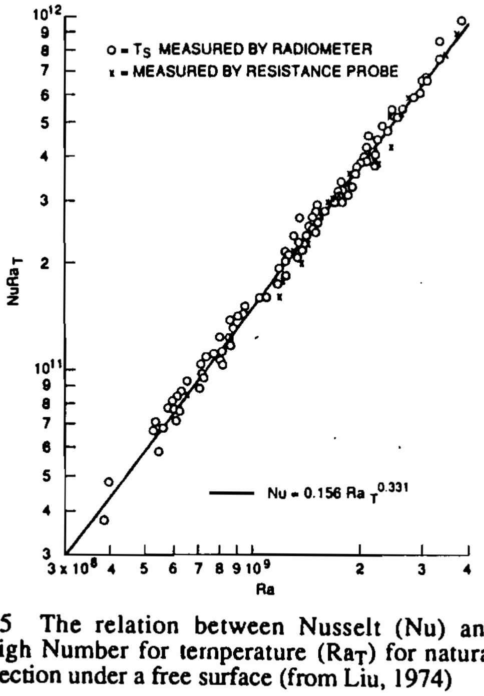

Fig 5 The relation between Nusselt (Nu) and Raleigh Number for temperature (Ra_T) for natural convection under a free surface (from Liu, 1974)

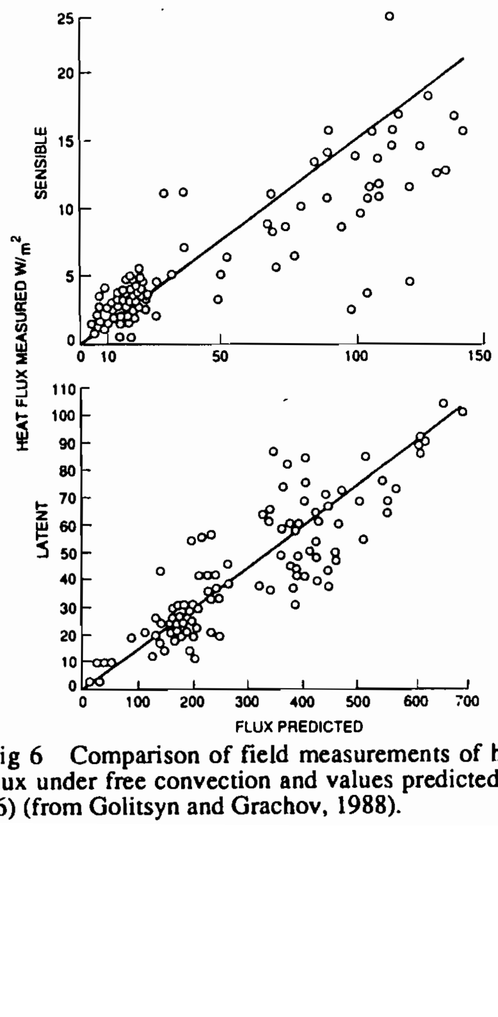

Fig 6 Comparison of field measurements of heat flux under free convection and values predicted by (6) (from Golitsyn and Grachov, 1988).

$$H = A\rho c\left(\frac{\alpha g \kappa_T^2}{\nu}\right)^{1/3} \Delta T^{4/3} \tag{5}$$

The relation between Q and ΔT is independent of the depth of fluid. For a inhomogeneous fluid like the atmosphere over ocean, (4) can be generalized to include moisture transport,

$$Nu = A\left[Ra_T + Ra_Q\left(\frac{Pr}{Sc}\right)^{3/2}\right]^{1/3} \tag{6a}$$

$$Sh = A\left[Ra_Q + Ra_T\left(\frac{Sc}{Pr}\right)^{3/2}\right]^{1/3} \tag{6b}$$

where $Sh \equiv Ed/(\rho\kappa_Q\Delta Q)$ is the Sherwood number, $Sc=\nu/\kappa_Q$ is the Schmidt number, κ_Q is the diffusivity of water vapor, $Ra_Q \equiv \beta g \Delta Q d^3/\kappa_Q \nu$ is the Raleigh number for humidity, and β is the expansion coefficient due to water vapor. The heat and moisture fluxes can be reduced to functions of ΔT and ΔQ. Fig. 6, from Golitsyn and Garchov (1986), compared field measurements of heat and moisture fluxes to those predicted by (6).

Wyngaard et al. (1971) recognized that the similarity theory breaks down when there is no mean wind and introduce a free convection scale for the atmospheric mixed layer with depth d

$$U_f = \left(\frac{\alpha g d H}{c\rho}\right)^{1/3} \tag{7}$$

and Businger (1973) postulated that convection will induce local surface friction velocity, U_* and U_*/U_f is a decreasing function of d/z_o. Assuming

$$\frac{U_*}{U_f} \propto \left(\frac{d}{z_o}\right)^{-1/3} \tag{8}$$

and that the resident time scale of the fluid at the surface is equal to the Kolmogorov time scale, Liu et al. (1979) derived (4) from (8). Schuman (1988) suggested that (4) is applicable only to smooth flow. In rough flow, he suggested

$$Nu = A\, Ra_T^{1/2} \tag{10}$$

Under free convection conditions, the flow is always smooth over the ocean. The independence of heat flux from any depth scale,as in (6), remains to be vigorously tested.

4. LATENT HEAT FLUX FROM SATELLITE DATA

Of the three parameters required to compute LE, spaceborne sensors can measure T_s and U, but cannot measure Q. It was found that at the monthly time scale, atmospheric water has a single dominant mode of variability and Q can be derived from the columnar water vapor (W) measured by microwave radiometers. A statistical Q-W relation was established using 17 years of radiosonde reports from mid-ocean meteorological stations (Liu, 1986). This relation was found to be adequate in describing the seasonal and interannual variations over global oceans except in high latitudes during summer, with accuracy estimated to be 0.4-0.8 g/kg. With this relation, monthly fields of LE from 1980 to 1983 in the tropical Pacific were computed using data from Nimbus/SMMR. In comparison with monthly data from equatorial moorings and atolls, the scatters were found to be 0.6 m/s in U, 0.8°C in T_s and 0.4 g/kg in Q. The random error in LE is estimated to be 26 W/m^2 (Liu, 1988). The errors for T_s and LE were likely to be overestimated since a 200x200 km satellite average was compared with a spot measurement in an area of very large meridional gradient.

Fig. 7 shows the time-longitude distribution of T_s, U, W, and LE centered on the equator between 90°W and the date-line. The 1982-83 ENSO episode is envisioned as an apparent eastward migration of the warm water pool marked by the 28°C isotherm starting in June 1982. This results in a reverse of zonal T_s gradient near the date-line. The organized deep convection marked by high W also moves east from the date-line starting June 1982, leaving dry air behind. The seasonal cycle of U is disrupted by the eastward migration of low wind center representing surface convergence associated with the organized convection at the eastern terminal of anomalous westerlies. During April 1983, zonal belts of high T_s, high W and low U stretch across the entire equatorial Pacific. Detailed evolution of these three parameters during the episode is described in Liu (1989a). Despite the warm water, LE is below normal due mainly to the low U near the convergence center. The annual October high does not reach the expected level.

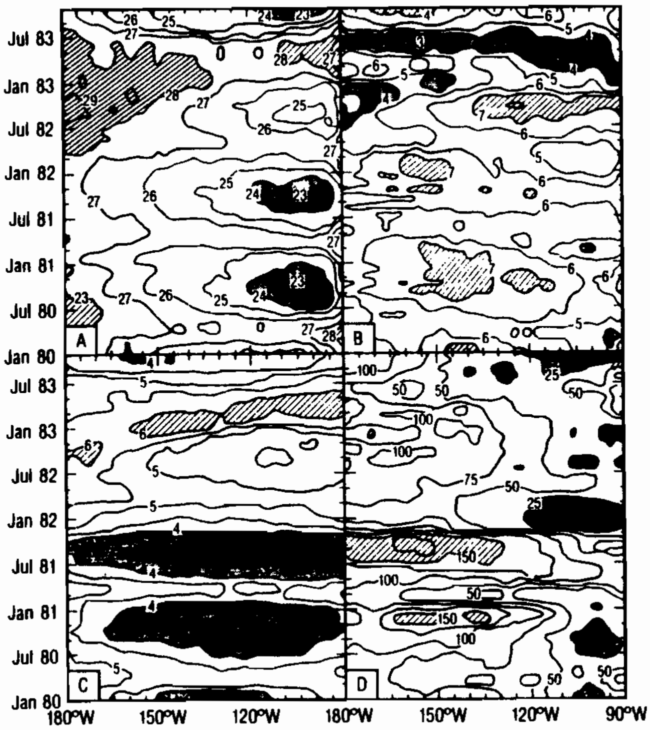

Fig.7 Time-longitude variation, centered on the equator, of (A) sea surface temperature, (B) surface wind speed, (C) columnar water vapor, and (D) latent heat flux. The intervals between isolines are 1°C, 1m/s, 0.5 g/cm^2, and 25 W/m^2 respectively.

The change of heat storage in the upper ocean is governed by the balance of heat gain from the surface and the loss through ocean dynamics. Fig. 8A shows the distribution of the contemporary correlation coefficient, at 2° latitude by 2° longitude grids, between LE and the time rate of change of sea surface temperature ($\partial T_s/\partial t$) for the period between February 1980 and September 1983, including an intense El Nino and Southern Oscillation episode. The gradient of the linear regression for three consecutive months of T_s is used to represent $\partial T_s/\partial t$. The 44 months of LE and $\partial T_s/\partial t$ fields were reconstructed from the first three empirical orthogonal functions accounting for 60% and 83% of the variance respectively. The low correlation in the near equatorial regions (left) is due the cloud and insolation variabilities in areas of organized convection and surface convergence (e.g., ITCZ) and due to ocean upwelling (along the equator). Off phase moisture variation is likely to be cause of low correlation at 20°N. Outside of these regions, the correlations are significant, indicating dominant influence of surface latent heat flux in upper ocean heat balance. By adding the surface shortwave radiation derived from observations from the VISSR (Visible Infrared Spin Scan Radiometer) (Liu and Gautier, 1989) to the latent heat flux, the area of low correlation is concentrated in a narrow belt around the equator (Fig. 8B) showing that in this equatorial wave guide, ocean dynamics plays a dominant role.

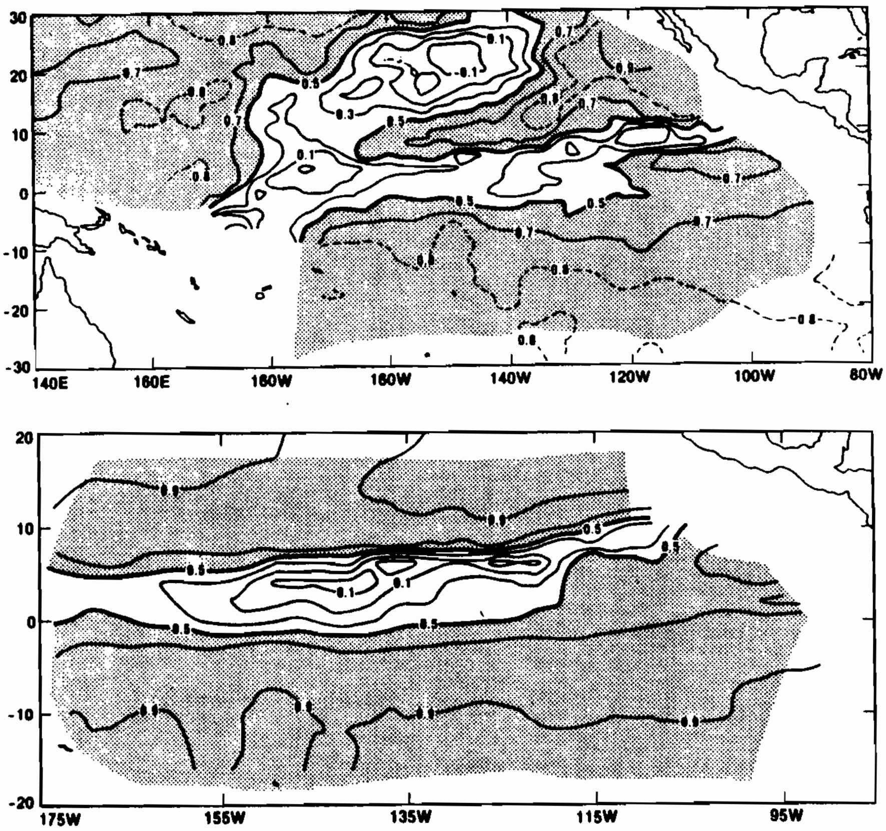

Fig. 8 Contemporary correlation coefficient between time rate of change of sea surface temperature and (A) latent heat flux (top), and (B) net heat flux (bottom). Solid isolines have 0.2 intervals.

5. CONCLUSION

C_E is constant only as a crude approximation. Most values used in the past led to underestimation of E in the western tropical Pacific (where winds are very light) because they do not account for the smooth flow characteristic of increasing values with decreasing winds and they neglect the moisture-induced instability. A scheme for parameterization under free convection is also described which still needs further validation. Inhomogeneous and non-stationary conditions, related to thermal plumes or convection, are not addressed and required more studies and scrutiny.

A method of estimating E with observations from spaceborne microwave is described. Application has been confined to monthly means but extension of the technique to higher temporal frequencies is being explored (Liu, 1989b). Combination of LE with surface shortwave radiation demonstrated the ocean's response to surface thermal forcing.

ACKNOWLEGMENTS

This study was performed at the Jet Propulsion Laboratory, California Institute of Technology, under contract with the National Aeronautic and Space administration. The computation of net heat flux is part of the TOGA Heat Exchange Project, an interagency supported research program.

References

Anderson, R.J. and S.D. Smith, 1981: Evaporation coefficient for the sea surface from eddy flux measurements, *J. Geophys. Res.*, *86*, 449-459.
Bradley, E.F., P.A. Coppin, and J.S. Godfrey, 1989: Measurements of heat and moisture fluxes from the western tropical Pacific Ocean. This Proceeding.
Businger, J.A., 1973: A note on free convection. *Boundary Layer Meteor.*, *4*, 323-326.
Bunker, A.F., 1976: Computations of surface energy flux and annual air-sea interaction cycles of the North Atlantic Ocean, *Mon. Wea. Rev.*, *104*, 1122-1140.
Charnock, H., 1955: Wind stress on a water surface. *Quart. J. Roy. Meteor. Soc.*, *81*, 639-640.
Deardorff, J.W., 1968: Dependence of air-sea transfer coefficients on bulk stability. *J. Geophys. Res.*, *73*, 2549-2557.
Deissler, R.G., and C.S. Eian, 1952: Analytical and experimental investigation of fully developed turbulent flow of air in a smooth tube with heat transfer with variable fluid properties. *NACA Tech. Note 2629*.
Golitsyn, G.S., and A.A. Grachov, 1986: Free convection of multi-component media and parameterization of air-sea interaction at light winds. *Ocean-Air Interactions*, *1*, 57-78.
Hsiung, J., 1986: Mean surface energy fluxes over the global ocean. *J. Geophys. Res.*, *91*, 10585-10606.
Kondo, J., Y. Fujinawa, and G. Naito, 1973: High frequency component of ocean waves and their relation to aerodynamic roughness. *J. Phys. Oceanogr.*, *3*, 197-202.
Krishnamurti, R., 1973: Further studies on transition to turbulent convection. *J. Fluid Mech.*, *60*, 285-303.
Large, R.G. and S. Pond, 1982: Sensible and latent heat flux measurements over the ocean, *J. Phys. Oceanogr.*, *12*, 464-482.

Liu, W.T., 1974: *Thermal Structure and Heat Transport in the Molecular Boundary Layer under an Evaporating Surface of a Deep Tank of Water.* Master Thesis, University of Washington.

Liu, W.T., 1978: *The Molecular Effects on Air-sea Exchanges.* Ph.D. dissertation, University of Washington.

Liu, W.T., 1986: Statistical relation between monthly precipitable water and surface-level humidity over global oceans. *Mon. Wea. Rev., 114,* 1591-1602.

Liu, W.T., 1988: Moisture and latent heat flux variabilities in the tropical Pacific derived from satellite data. *J. Geophys. Res., 93,* 6749-6760, 6965-6968.

Liu, W.T., 1989a: The annual and interannual variabilities of precipitable water, surface wind speed, and sea surface temperature, over the tropical Pacific. *Ocean Air Interaction,* in press.

Liu, W.T., 1989b: Remote sensing of surface turbulence heat flux. *Surface Waves and Fluxes: Current Theory and Remote Sensing,* Chapter 16, G. Geerneart (ed.), Reidel Publishing Co.

Liu, W.T., C. Gautier., 1989: Remote sensing of the thermal forcing on the tropical Pacific. *Proc. of IGARSS 89,* to appear.

Liu, W.T., K.B. Katsaros, and J.A. Businger, 1979: Bulk parameterization of air-sea exchanges of heat and water vapor including the molecular constraints at the surface, *J. Atmos. Sci., 36,* 1722-1735.

Nikuradse, J., 1933: Stromungsgesetze in Raubven Rohren. *V.D.I. Forschungsheft 361.*

Reichartdt, H., 1940: Die Warmeubertragung in turbulenten Reibungsschichten Z. *Angew. Math. Mech., 20,* 297-328.

Schlichting, H., 1968: *Boundary Layer Theory,* McGraw Hill, New York.

Schumann, U., 1988: Minimum friction velocity and heat transfer in the rough surface layer of a convective boundary layer. *Bound. Layer Meteor., 44,* 311-326.

Wyngaard, J.C., Cote, O.R., and Izumi, Y., 1971: Local free convection, similarity and budgets of shear stress and heat flux. *J. Atmos. Sci., 28,* 1171-1182.

WESTERN PACIFIC INTERNATIONAL MEETING AND WORKSHOP ON TOGA COARE

Nouméa, New Caledonia
May 24-30, 1989

PROCEEDINGS

edited by

Joël Picaut *
Roger Lukas **
Thierry Delcroix *

* ORSTOM, Nouméa, New Caledonia
** JIMAR, University of Hawaii, U.S.A.

INSTITUT FRANÇAIS DE RECHERCHE SCIENTIFIQUE
POUR LE DÉVELOPPEMENT EN COOPÉRATION

ORSTOM

Centre de Nouméa

TABLE OF CONTENTS

ABSTRACT i

RESUME iii

ACKNOWLEDGMENTS vi

INTRODUCTION

1. Motivation 1
2. Structure 2

LIST OF PARTICIPANTS 5

AGENDA 7

WORKSHOP REPORT

1. Introduction 19
2. Working group discussions, recommendations, and plans 20
   a. Air-Sea Fluxes and Boundary Layer Processes 20
   b. Regional Scale Atmospheric Circulation and Waves 24
   c. Regional Scale Oceanic Circulation and Waves 30
3. Related programs 35
   a. NASA Ocean Processes and Satellite Missions 35
   b. Tropical Rainfall Measuring Mission 37
   c. Typhoon Motion Program 39
   d. World Ocean Circulation Experiment 39
4. Presentations on related technology 40
5. National reports 40
6. Meeting of the International Ad Hoc Committee on TOGA COARE 40

APPENDIX: WORKSHOP RELATED PAPERS

Robert A. Weller and David S. Hosom: Improved Meteorological Measurements from Buoys and Ships for the World Ocean Circulation Experiment 45

Peter H. Hildebrand: Flux Measurement using Aircraft and Radars 57

Walter F. Dabberdt, Hale Cole, K. Gage, W. Ecklund and W.L. Smith: Determination of Boundary-Layer Fluxes with an Integrated Sounding System 81

MEETING COLLECTED PAPERS

WATER MASSES, SEA SURFACE TOPOGRAPHY, AND CIRCULATION

Klaus Wyrtki: Some Thoughts about the West Pacific Warm Pool 99
Jean René Donguy, Gary Meyers, and Eric Lindstrom: Comparison of the Results of two West Pacific Oceanographic Expeditions FOC (1971) and WEPOCS (1985-86) 111
Dunxin Hu, and Maochang Cui: The Western Boundary Current in the Far Western Pacific Ocean 123
Peter Hacker, Eric Firing, Roger Lukas, Philipp L. Richardson, and Curtis A. Collins: Observations of the Low-latitude Western Boundary Circulation in the Pacific during WEPOCS III 135
Stephen P. Murray, John Kindle, Dharma Arief, and Harley Hurlburt: Comparison of Observations and Numerical Model Results in the Indonesian Throughflow Region 145
Christian Henin: Thermohaline Structure Variability along 165°E in the Western Tropical Pacific Ocean (January 1984 - January 1989) 155
David J. Webb, and Brian A. King: Preliminary Results from Charles Darwin Cruise 34A in the Western Equatorial Pacific 165
Warren B. White, Nicholas Graham, and Chang-Kou Tai: Reflection of Annual Rossby Waves at The Maritime Western Boundary of the Tropical Pacific 173
William S. Kessler: Observations of Long Rossby Waves in the Northern Tropical Pacific 185
Eric Firing, and Jiang Songnian: Variable Currents in the Western Pacific Measured During the US/PRC Bilateral Air-Sea Interaction Program and WEPOCS 205
John S. Godfrey, and A. Weaver: Why are there Such Strong Steric Height Gradients off Western Australia ? 215
John M. Toole, R.C. Millard, Z. Wang, and S. Pu: Observations of the Pacific North Equatorial Current Bifurcation at the Philippine Coast 223

EL NINO/SOUTHERN OSCILLATION 1986-87

Gary Meyers, Rick Bailey, Eric Lindstrom, and Helen Phillips: Air/Sea Interaction in the Western Tropical Pacific Ocean during 1982/83 and 1986/87 229
Laury Miller, and Robert Cheney: GEOSAT Observations of Sea Level in the Tropical Pacific and Indian Oceans during the 1986-87 El Nino Event 247
Thierry Delcroix, Gérard Eldin, and Joël Picaut: GEOSAT Sea Level Anomalies in the Western Equatorial Pacific during the 1986-87 El Nino, Elucidated as Equatorial Kelvin and Rossby Waves 259
Gérard Eldin, and Thierry Delcroix: Vertical Thermal Structure Variability along 165°E during the 1986-87 ENSO Event 269
Michael J. McPhaden: On the Relationship between Winds and Upper Ocean Temperature Variability in the Western Equatorial Pacific 283

John S. Godfrey, K. Ridgway, Gary Meyers, and Rick Bailey: Sea Level and Thermal Response to the 1986-87 ENSO Event in the Far Western Pacific ... 291
Joël Picaut, Bruno Camusat, Thierry Delcroix, Michael J. McPhaden, and Antonio J. Busalacchi: Surface Equatorial Flow Anomalies in the Pacific Ocean during the 1986-87 ENSO using GEOSAT Altimeter Data ... 301

THEORETICAL AND MODELING STUDIES OF ENSO AND RELATED PROCESSES

Julian P. McCreary, Jr.: An Overview of Coupled Ocean-Atmosphere Models of El Nino and the Southern Oscillation ... 313
Kensuke Takeuchi: On Warm Rossby Waves and their Relations to ENSO Events ... 329
Yves du Penhoat, and Mark A. Cane: Effect of Low Latitude Western Boundary Gaps on the Reflection of Equatorial Motions ... 335
Harley Hurlburt, John Kindle, E. Joseph Metzger, and Alan Wallcraft: Results from a Global Ocean Model in the Western Tropical Pacific ... 343
John C. Kindle, Harley E. Hurlburt, and E. Joseph Metzger: On the Seasonal and Interannual Variability of the Pacific to Indian Ocean Throughflow ... 355
Antonio J. Busalacchi, Michael J. McPhaden, Joël Picaut, and Scott Springer: Uncertainties in Tropical Pacific Ocean Simulations: The Seasonal and Interannual Sea Level Response to Three Analyses of the Surface Wind Field ... 367
Stephen E. Zebiak: Intraseasonal Variability - A Critical Component of ENSO ? ... 379
Akimasa Sumi: Behavior of Convective Activity over the "Jovian-type" Aqua-Planet Experiments ... 389
Ka-Ming Lau: Dynamics of Multi-Scale Interactions Relevant to ENSO ... 397
Pecheng C. Chu and Roland W. Garwood, Jr.: Hydrological Effects on the Air-Ocean Coupled System ... 407
Sam F. Iacobellis, and Richard C.J. Somerville: A one Dimensional Coupled Air-Sea Model for Diagnostic Studies during TOGA-COARE ... 419
Allan J. Clarke: On the Reflection and Transmission of Low Frequency Energy at the Irregular Western Pacific Ocean Boundary - a Preliminary Report ... 423
Roland W. Garwood, Jr., Pecheng C. Chu, Peter Muller, and Niklas Schneider: Equatorial Entrainment Zone : the Diurnal Cycle ... 435
Peter R. Gent: A New Ocean GCM for Tropical Ocean and ENSO Studies ... 445
Wasito Hadi, and Nuraini: The Steady State Response of Indonesian Sea to a Steady Wind Field ... 451
Pedro Ripa: Instability Conditions and Energetics in the Equatorial Pacific ... 457
Lewis M. Rothstein: Mixed Layer Modelling in the Western Equatorial Pacific Ocean ... 465
Neville R. Smith: An Oceanic Subsurface Thermal Analysis Scheme with Objective Quality Control ... 475
Duane E. Stevens, Qi Hu, Graeme Stephens, and David Randall: The hydrological Cycle of the Intraseasonal Oscillation ... 485
Peter J. Webster, Hai-Ru Chang, and Chidong Zhang: Transmission Characteristics of the Dynamic Response to Episodic Forcing in the Warm Pool Regions of the Tropical Oceans ... 493

MOMENTUM, HEAT, AND MOISTURE FLUXES BETWEEN ATMOSPHERE AND OCEAN

W. Timothy Liu: An Overview of Bulk Parametrization and Remote Sensing of Latent Heat Flux in the Tropical Ocean ... 513
E. Frank Bradley, Peter A. Coppin, and **John S. Godfrey**: Measurements of Heat and Moisture Fluxes from the Western Tropical Pacific Ocean ... 523
Richard W. Reynolds, and **Ants Leetmaa**: Evaluation of NMC's Operational Surface Fluxes in the Tropical Pacific ... 535
Stanley P. Hayes, Michael J. McPhaden, John M. Wallace, and **Joël Picaut**: The Influence of Sea-Surface Temperature on Surface Wind in the Equatorial Pacific Ocean ... 543
T.D. Keenan, and **Richard E. Carbone**: A Preliminary Morphology of Precipitation Systems In Tropical Northern Australia ... 549
Phillip A. Arkin: Estimation of Large-Scale Oceanic Rainfall for TOGA ... 561
Catherine Gautier, and **Robert Frouin**: Surface Radiation Processes in the Tropical Pacific ... 571
Thierry Delcroix, and **Christian Henin**: Mechanisms of Subsurface Thermal Structure and Sea Surface Thermo-Haline Variabilities in the South Western Tropical Pacific during 1979-85 - A Preliminary Report ... 581
Greg. J. Holland, T.D. Keenan, and **M.J. Manton**: Observations from the Maritime Continent : Darwin, Australia ... 591
Roger Lukas: Observations of Air-Sea Interactions in the Western Pacific Warm Pool during WEPOCS ... 599
M. Nunez, and **K. Michael**: Satellite Derivation of Ocean-Atmosphere Heat Fluxes in a Tropical Environment ... 611

EMPIRICAL STUDIES OF ENSO AND SHORT-TERM CLIMATE VARIABILITY

Klaus M. Weickmann: Convection and Circulation Anomalies over the Oceanic Warm Pool during 1981-1982 ... 623
Claire Perigaud: Instability Waves in the Tropical Pacific Observed with GEOSAT ... 637
Ryuichi Kawamura: Intraseasonal and Interannual Modes of Atmosphere-Ocean System Over the Tropical Western Pacific ... 649
David Gutzler, and **Tamara M. Wood**: Observed Structure of Convective Anomalies ... 659
Siri Jodha Khalsa: Remote Sensing of Atmospheric Thermodynamics in the Tropics ... 665
Bingrong Xu: Some Features of the Western Tropical Pacific: Surface Wind Field and its Influence on the Upper Ocean Thermal Structure ... 677
Bret A. Mullan: Influence of Southern Oscillation on New Zealand Weather ... 687
Kenneth S. Gage, Ben Basley, Warner Ecklund, D.A. Carter, and**John R. McAfee**: Wind Profiler Related Research in the Tropical Pacific ... 699
John Joseph Bates: Signature of a West Wind Convective Event in SSM/I Data ... 711
David S. Gutzler: Seasonal and Interannual Variability of the Madden-Julian Oscillation ... 723
Marie-Hélène Radenac: Fine Structure Variability in the Equatorial Western Pacific Ocean ... 735
George C. Reid, Kenneth S. Gage, and **John R. McAfee**: The Climatology of the Western Tropical Pacific: Analysis of the Radiosonde Data Base ... 741

Chung-Hsiung Sui, and Ka-Ming Lau: Multi-Scale Processes in the Equatorial Western Pacific 747
Stephen E. Zebiak: Diagnostic Studies of Pacific Surface Winds 757

MISCELLANEOUS

Rick J. Bailey, Helene E. Phillips, and Gary Meyers: Relevance to TOGA of Systematic XBT Errors 775
Jean Blanchot, Robert Le Borgne, Aubert Le Bouteiller, and Martine Rodier: ENSO Events and Consequences on Nutrient, Planktonic Biomass, and Production in the Western Tropical Pacific Ocean 785
Yves Dandonneau: Abnormal Bloom of Phytoplankton around 10°N in the Western Pacific during the 1982-83 ENSO 791
Cécile Dupouy: Sea Surface Chlorophyll Concentration in the South Western Tropical Pacific, as seen from NIMBUS Coastal Zone Color Scanner from 1979 to 1984 (New Caledonia and Vanuatu) 803
Michael Szabados, and Darren Wright: Field Evaluation of Real-Time XBT Systems 811
Pierre Rual: For a Better XBT Bathy-Message: Onboard Quality Control, plus a New Data Reduction Method 823